Stress-strain state of fiber cement cladding within curtain wall system

D. Egorov[a*], A. Galyamichev[a], E. Gerasimova[b], D. Serdjuks[c]
[a] Peter the Great St. Petersburg Polytechnic University, St. Petersburg, Russia
[b] NIUPC «Mezhregional'nyj institut okonnyh i fasadnyh konstrukcij», St. Petersburg, Russia
[c] Riga Technical University, Riga, Latvia
* Email: egorov.dv@edu.spbstu.ru

Abstract. This article presents the experimental methodology and results of laboratory tests and numerical modeling in order to determine the values of bearing capacity and stiffness of fiber cement board (FCB) within a frame of curtain wall system. The performance of a panel as a part of a system is taken into account for evaluation of the stress-strain state of a cladding. An analysis included 2 stages: an experimental study of a full-size fragment of a curtain wall system with fiber cement cladding and its numerical simulation by means of finite element method (FEM). The dependences of the deflection of the panel on a value of uniformly distributed load were obtained, and the experimental results converged with numerical calculation. The maximum values of the uniformly distributed (simulating wind impact) loads acting on the panel under which the panel satisfies the requirements stated by Ultimate and Serviceability Limit States were calculated also. It can be concluded that onset of Ultimate Limit State is characterized by appearance of cracks due to the stresses in the panel exceeding the value of flexural strength in the area of fastening to curtain wall frame. The results demonstrated that the stress-strain state of the cladding depends on the structural scheme of the supporting frame of the curtain wall system and its rigidity, therefore it is recommended to perform tests on the cladding in conjunction with the supporting frame.

1. Introduction

Nowadays curtain wall systems are actively used in construction. Such systems became popular due to the fact that a large number of buildings no longer met the requirements stated by appeared regulatory documents. Renovation of facades by means of traditional methods was significantly less efficient and more expensive. A possibility to install such systems in any weather conditions, which is quite relevant for construction in areas of changeable climate, was an excellent advantage in addition. The curtain wall systems now possess structural importance equivalent to that gained by other structural elements of the building. A certain number of issues related to its application remain to be studied despite the fact that this material was in use since the 1990's. One of them is the development of testing and calculation methods of cladding as part of the curtain wall system, as well as the development of requirements for fastening this cladding to the supporting frame of the system.

Fiber cement board (FCB) is a flat rectangular product made of cellulose fibers, mineral aggregates and cement, with a flat or embossed front surface covered with protective and decorative polymer coating. These panels are used as cladding elements of the external and internal walls (except basement walls) of buildings and structures within curtain wall systems and as opaque elements in glass facades. The advantages and disadvantages of these panels are studied in article as a part of curtain wall systems [1]. Most common sizes of FCB vary in length from 1200 to 3600 mm, in width from 1120 to 1570 mm and a thickness of them is equal to 6, 8, 10, 12, 14 or 16 mm. The panels are fastened to the supporting structure by means of exhaust rivets and self-tapping screws or several types of hidden fixators (e.g., Keil anchors) in most of cases.

Boards with visible fastening by exhaust rivets to the metal supporting frame of curtain wall system were analyzed within this study. One of fastening points is fixed and the rest of them are movable (Fig. 1) in order

to prevent occurrence of stresses due to temperature deformations of the plate and the metal frame. At the moment, in many technical certificates and installation guidelines for curtain wall system with fiber cement cladding, the critical rivet installation step is presumed to be equal to 600 mm, the edge distances in transverse and longitudinal directions are 30 mm and 50−150 mm respectively.
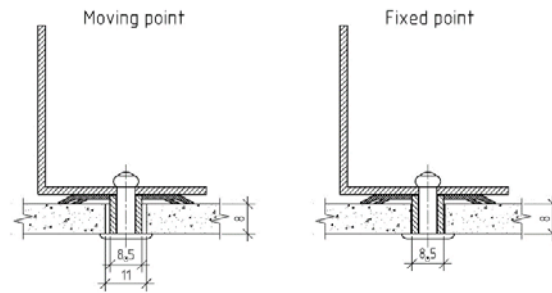

Figure 1. Fastening points of fiber cement board to the supporting frame.

According to their mechanical and deformation characteristics and due to their structure, FCBs are anisotropic material with different characteristics across and along the fibers. The works [2–7] are devoted to the analysis and improvement of the mechanical properties of fiber cement cladding. In [8], the effect of freeze-thaw cycles is considered, and in [9], influence of thermal impact on the properties of the boards is studied. Article [10] presents the results of the tests performed on cement boards with cellulose fibers as a reinforcing material in wet and dry conditions and determines the influence of the moisture rate on blast strength, ductility, bending strengths and other properties of FCBs.

Article [11] presents results of studies on fracture processes in FCBs and the use of non-destructive acoustic emission method and time-frequency analysis for testing FCBs.

In order to design curtain wall system, which fully satisfies the performance requirements during operation, it is necessary to properly calculate its cladding. The calculation should include verification according to both Ultimate Limit State (ULS) and Serviceability Limit State (SLS). Therefore, there is a need in development of a laboratory test and design method for the cladding as part of the curtain wall system, as well as the requirements for its fastening. Similar full-size tests were already performed on glass and thin ceramic panels [12–14]. In [15], elements of filling are taken into account for numerical modeling of translucent facade structures.

Loads and effects acting on the structure remain an important factor, which needs to be taken into account for reliable calculations of curtain wall systems. Loads acting on facade structures in accordance with Limit State Design are described in [16, 17]. Article [18] analyses the procedure of numerical modeling of the cladding panel by FEM. Article [19] verifies the possibility of usage of FCBs as a cladding in lightweight structures. Calculation methods, considering joint performance of structural members, are studied in [20].

The aim of this study was to determine the stress-strain state of fiber cement panels as part of curtain wall system subjected to a uniformly distributed load.

The study was divided into several stages:

1. An experimental study of a full-sized fragment of a curtain wall system with fiber cement cladding.

2. Numerical modeling of the facade fragment by means of FEM realized in SCAD Office software package.

3. Comparison of the results obtained through numerical modeling and experimental study.

The subjects of the study were:

- The value of uniformly distributed load, which leads to the loss of the bearing capacity of FCB under the given conditions of fastening;

- The values of the deflection at the characteristic points of the panels as a result of the action of a uniformly distributed load;

- The character of a panel failure due to limit state occurrence;

- The possibility of usage of FCBs in terms of bearing capacity with a distance between adjacent fastening points more than 600 mm;

- The possibility of usage of FCBs in terms of bearing capacity with a distance from the edge of the panel to the axis of the fastening installation hole equal to 30 mm.

2. Materials and Methods

2.1. Experimental study of FCBs within curtain wall system

The experimental method included a set of the tests on full-size fragments of a curtain wall system with cladding made of FCBs in laboratory conditions. Test bench implied the installation of a fragment in a horizontal position (Fig. 2), and application of the load simulating the most unfavorable type of impact for a given design solution − wind load from leeward side of the building, under which the panel bends with simultaneous separation from the frame of system.

The object of current study was fiber cement panels with thickness of 8 and 10 mm painted on the front surface. The considered panels had geometric dimensions of 3600×1500 mm and were installed as cladding in curtain wall system.
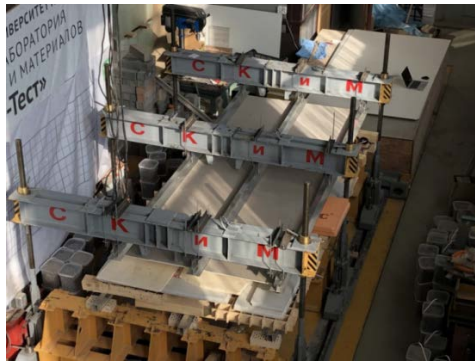

Figure 2. Initial position of the sample on the test bench.

The bearing frame was a system designed for façade cladding by means of sheet panels. The system consisted of a subframe and brackets. Three crossbeams of increased rigidity acted as the supporting base, to which the brackets of the curtain wall system were clamped by an angle profile and threaded rods. The brackets were installed with a step *a* of 1770 mm and *b* of 720 mm (Fig. 3), and the subframes were creating two-span continuous scheme, in order to obtain the most general case of curtain wall system. The fixation of the subframe profiles to the brackets was carried out by rivets, the number of which depends on the type of bracket: 8 rivets were used for the bearing bracket, and 4 rivets for the supporting.
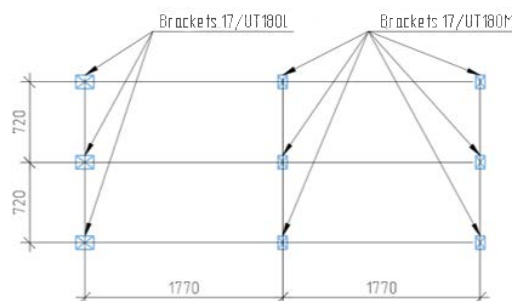

Figure 3. Arrangement of brackets for subframe attachment.

Figure 4. Attachment of brackets to traverses and fixation of the subframe to the brackets.

The FCB was connected to the subframe by rivets installed in pre-drilled holes together with polyamide sleeves. The installation step for fasteners (rivets) in the longitudinal direction (along the larger side) was taken as 708 mm and in the transverse direction as 720 mm, within this study. The distance from the edge of the panel to the axis of the hole for mounting the fastener was equal to 30 mm both in the longitudinal and transverse directions (Fig. 5).

Three dial indicators with an accuracy of 0.01 mm installed at the characteristic points of the structure (Fig. 5) allowed to obtain the values of vertical displacements of the panel. The indicator DI1 was installed at

the point where the maximum vertical displacements of the fiber cement panel were observed, the indicator DI2 showed the joint´s displacements of the FCB and the middle subframe profile, and the indicator DI3 tracked the displacements of the edge of the panel together with the subframe profile.
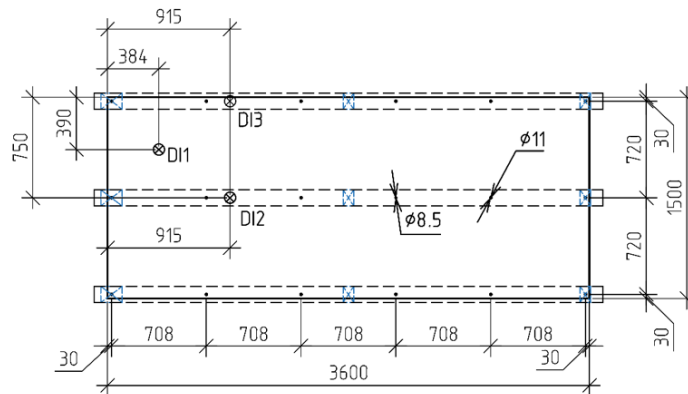

Figure 5. The position of the holes and dial indicators on the test fragment.

Uniformly distributed load was realized through placement of equal loads with weight of 7.5 kg each, located on the surface of the panel in a certain sequence (Fig. 6, 7). Initial load of 22 kg/m³ was applied in order to remove backlash in the mounted structure of the curtain wall system. After that, the load was eliminated and the initial parameters of the dial indicator were recorded for the following calculation of the vertical displacements of the cladding panel. Sequential loading was carried out with simultaneous recording of the deflection values until the panel was fractured or cracks appeared on its outer surface.
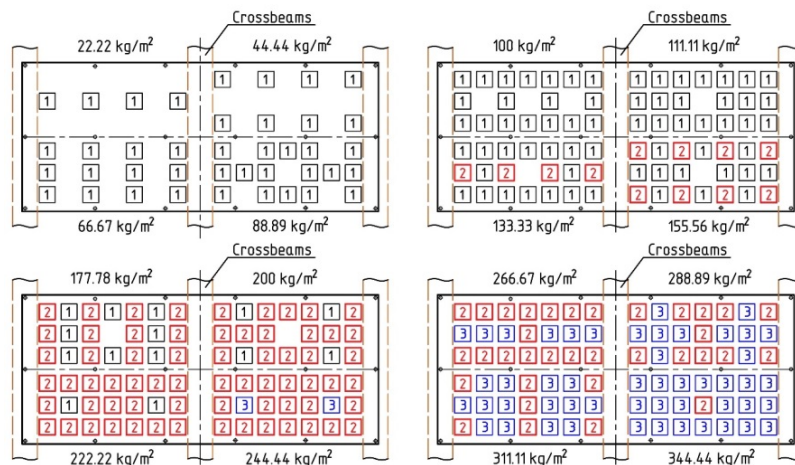

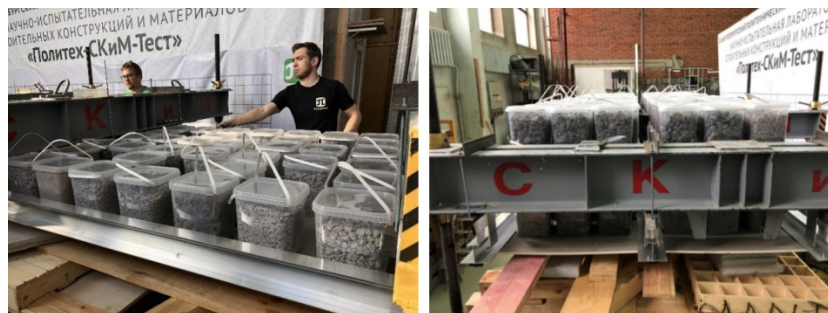**Figure 6. Load distribution on the panel (number indicates the quantity of loads placed one over the other).**

Figure 7. Application of distributed load during the test: left – 100 kg/m²; right − 344.44 kg/m².

2.2. Numerical modeling of FCBs within curtain wall system

Procedure of numerical modeling included the following tasks:

1. Determination of the displacements of the curtain wall system jointly with the cladding panels under the action of uniformly distributed and concentrated load, which was representing uniformly distributed load during the experimental study.

2. Determination of stresses in the cladding panel under the action of uniformly distributed load and verification of the panel in accordance with ULS.

3. Determination the vertical displacements of the cladding panel without taking into account the displacements of the subsystem and verification of the panel in accordance with SLS.

Numerical modeling and static calculation of the cladding jointly with subframe profiles were performed using the finite element method (FEM) implemented in the SCAD Office 21.1 software package.

Metal elements were simulated by one-dimensional finite elements (beams), and the panel was simulated by two-dimensional finite elements (shells). The scheme of the fragment of the curtain wall system is shown in Fig. 8, in which the guide profiles are continuous two-span beam on hinged supports. The hinge support is made along the X and Y axis (in the plane of the facade), and in the Z direction the connection with the finite stiffness is modeled.
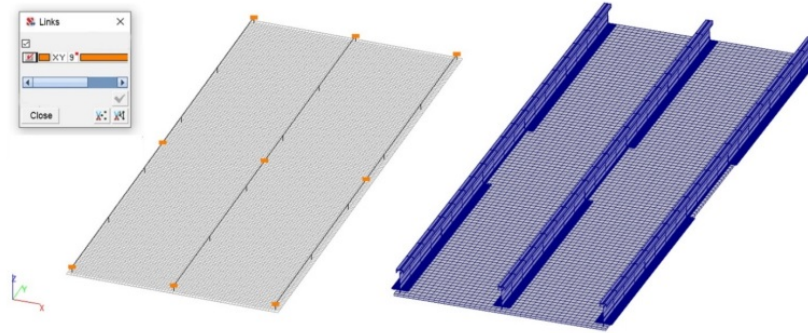

**Figure 8. Left - calculation scheme of the curtain wall system,
right - calculation model in the SCAD Office.**

System stiffness was determined on the base of test results in accordance with the formula:

$$K = \frac{R_z}{f} \tag{1}$$

Where R_z is the support reaction that occurs in the bracket as a result of the load applied during the test (obtained through static calculation in SCAD):

$$R_z = 66.15 \, kg$$

f is a displacement of the central support (obtained through the test with subframe profiles application):

$$f = 0.37 \, mm$$

$$K = \frac{66.15}{0.37} = 178.78 \, kg / mm$$

The panel is fastened to the subframe by hinges, which allow rotation from the plane of the panels and displacement in the plane of the facade (Fig. 9). A fixed fastening point allowed rotation in the plane of the panel and prevented linear displacements in the plane of the facade. Due to the strengthening of the frictional connection between the panel and subframe, jamming in the corresponding direction, which prevented linear and angular displacements, was created at the edge and corner fastening points.
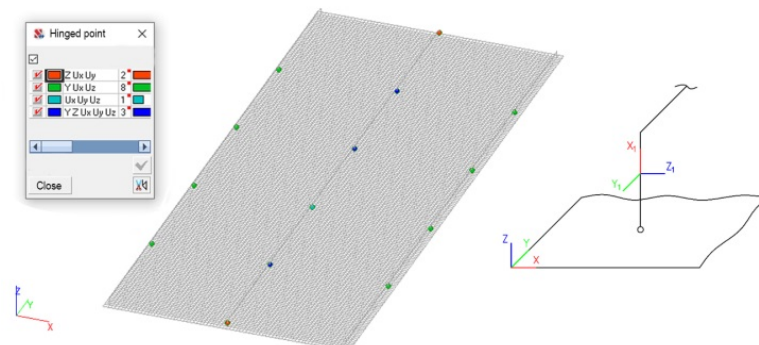

Figure 9. Hinges in the locations of fastening to the subframe profile (local coordinate system).

The reduction of the cross-section of subframe profile and the subsequent calculation of its modified geometric characteristics was performed with consideration of possible local buckling of individual elements subjected to normal compressive stresses.

The geometric characteristics of the cross-section before and after reduction were determined in the SCAD Office 21.1 software package (KONSUL satellite). The initial and final cross-sections are shown in Fig, 10.
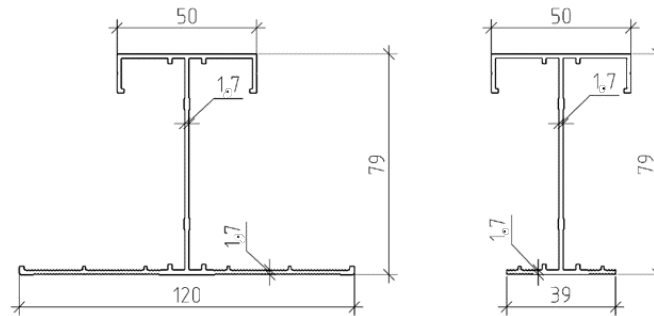

Figure 10. Cross-section of the subframe profile:
left – before reduction, right – after reduction of the lower part of cross-section
under its compression.

Stiffness characteristics of aluminum subframe profiles: modulus of elasticity is equal to $7.1 \cdot 10^9$ kg/m³; Poisson's ratio is equal to 0.3.

Flexural modulus of FCB:

$$E = 14000 \; MPa$$

Poisson's ratio of FCB:

$$v = 0.2$$

Panel's thicknesses:

$$t = 8 \; mm; t = 10 \; mm$$

A set of concentrated loads, which were applied during the test, was simulated as uniformly distributed loads on certain areas corresponding to actual location of single loads (Fig. 11), and their value was determined by the formula:

$$q = \frac{P_{load}}{S} \tag{2}$$

where P_{load} is a load unit weight:

$$P_{load} = 7.5 \; kg$$

S is the area of load unit in contact with panel surface, calculated for assumed FE mesh;

$$S = 0.16 \cdot 0.159 = 0.02544 \; m^2$$

$$q = \frac{7.5}{0.02544} = 294.81 \; kg / m^2$$

Thus, load distribution for each stage of application in numerical model corresponded to actual load application of experimental study.
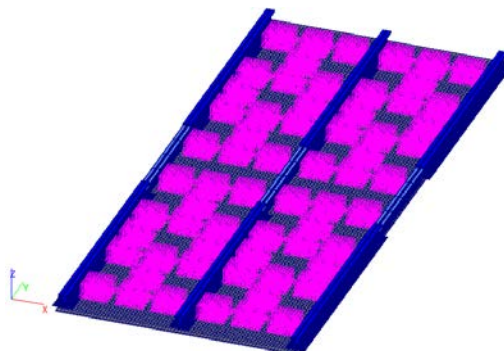

Figure 11. Load application (88.89 kg/m²) in numerical model.

3. Results and Discussion

3.1. Results of experimental study of FCBs within curtain wall system

Vertical displacements of the panel characteristic points were calculated on the base of dial indicator measurements and displayed in a form of graphs showing dependence of deflections on the applied load (Fig. 12−14).
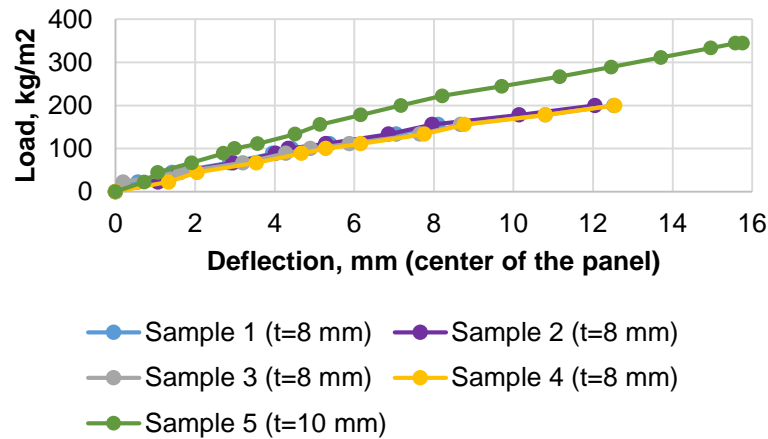

Figure 12. Deflection of the center of the panel under the action of applied load for the panels with the different thicknesses.
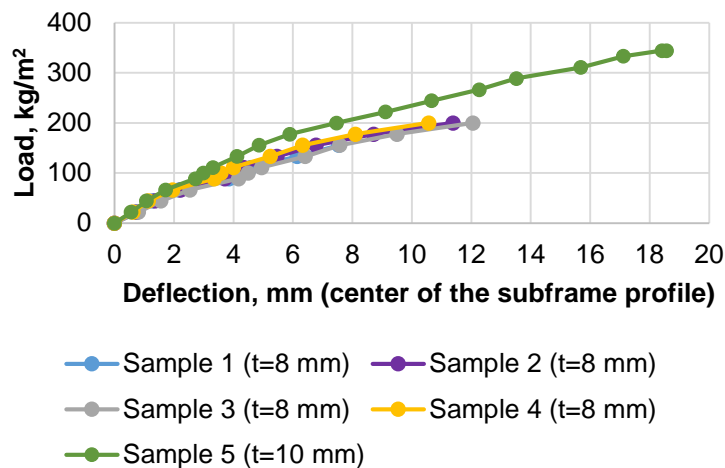

Figure 13. Deflection of the center of the subframe profile under the action of applied load for the panels with the different thicknesses.
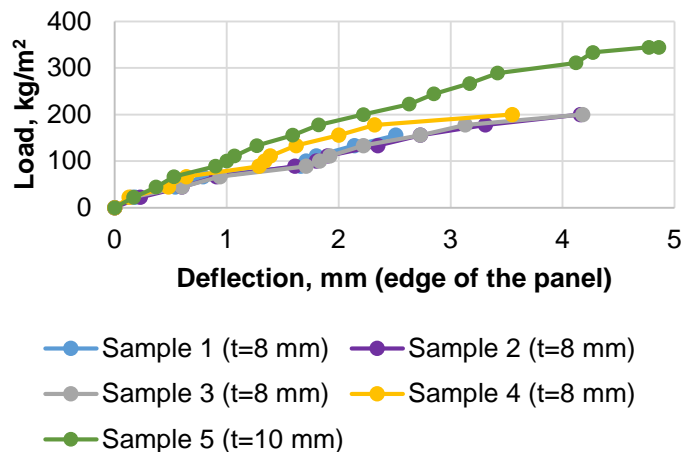

Figure 14. Deflection of the edge of the panel under the action of applied load for the panels with the different thicknesses.

Fracture of the panel was characterized by the formation of a longitudinal crack near the most loaded fastening point (Fig. 15), and the panel was destroyed by bending (Fig. 16) during subsequent loading.

Figure 15. Crack formation: left – sample 1 under the load of 155.56 kg/m^2; right – sample 2 under the load of 200 kg/m^2.

Figure 16. Fracture of the panel: left – sample 3 under the load of 222.22 kg/m^2; right – sample 4 under the load of 200 kg/m^2.

Fig. 17 demonstrates formation and opening of the crack in the corner of the panel under the load of 266.67 kg/m^2. However, the panel withstood loading up to the value of 344.44 kg/m^2. (Fig. 18), and fractured along the fibers near the central subframe profile, in the same way as in other tests.

Figure 17. Left – the formation and opening of a crack in sample 5 under the load of 266.67 kg/m^2; right – corner fastening point after the panel fracture.

Figure 18. Panel fracture of the sample 5 under the load 344.44 kg/m^2.

Plastic deformations of the central subframe profile in the area of the fastening point to the central support bracket are shown in Fig. 19. The numerical values of this deformation were measured during subsequent tests and allowed to calculate rigidity of this joint for further implementation in the numerical model.
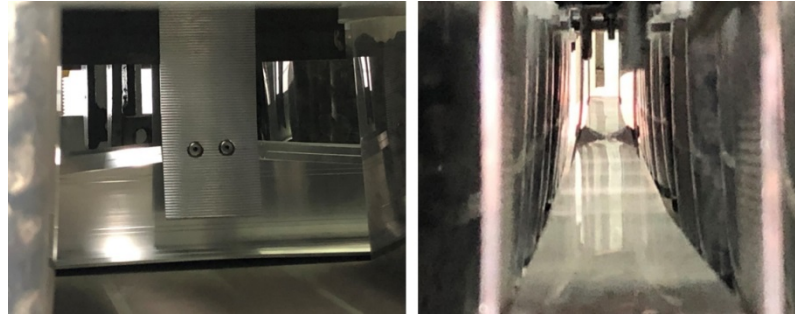
Figure 19. Deformation of the subframe profile in the area of the central bracket under the load of 344.44 kg/m² (sample 5).

3.2. Results of numerical modeling of FCBs within curtain wall system

Vertical displacements of the panel characteristic points were calculated according to results of numerical modeling and displayed in a form of graphs showing dependence of deflections on the applied load (Fig. 20–22).
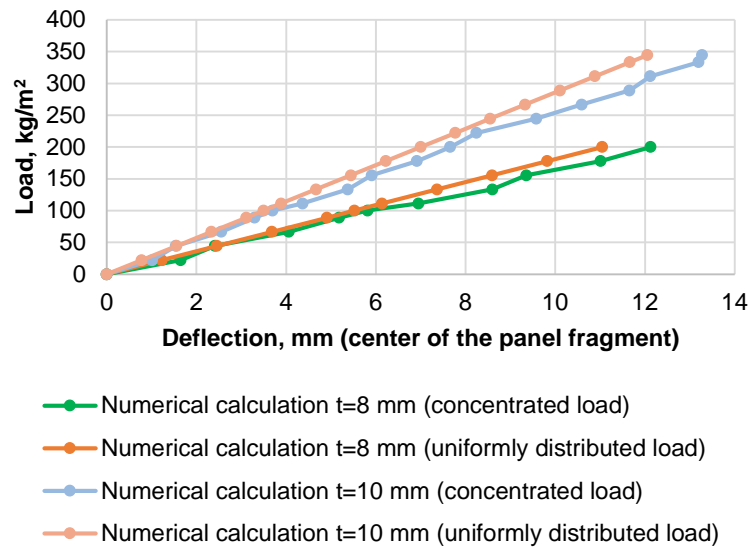

—●— Numerical calculation t=8 mm (concentrated load)
—●— Numerical calculation t=8 mm (uniformly distributed load)
—●— Numerical calculation t=10 mm (concentrated load)
—●— Numerical calculation t=10 mm (uniformly distributed load)

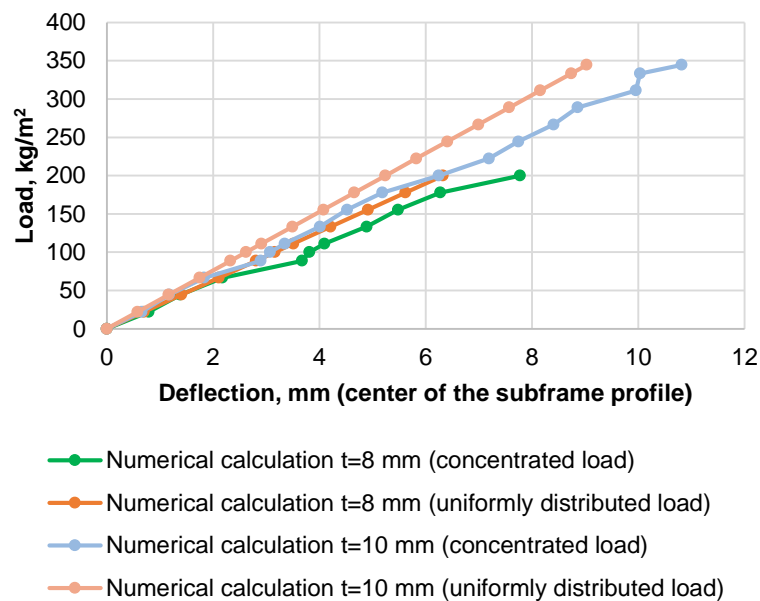**Figure 20. Deflection of the center of the panel fragment for the panels with the different thicknesses.**

—●— Numerical calculation t=8 mm (concentrated load)
—●— Numerical calculation t=8 mm (uniformly distributed load)
—●— Numerical calculation t=10 mm (concentrated load)
—●— Numerical calculation t=10 mm (uniformly distributed load)

Figure 21. Deflection of the center of the subframe profile for the panels with the different thicknesses.

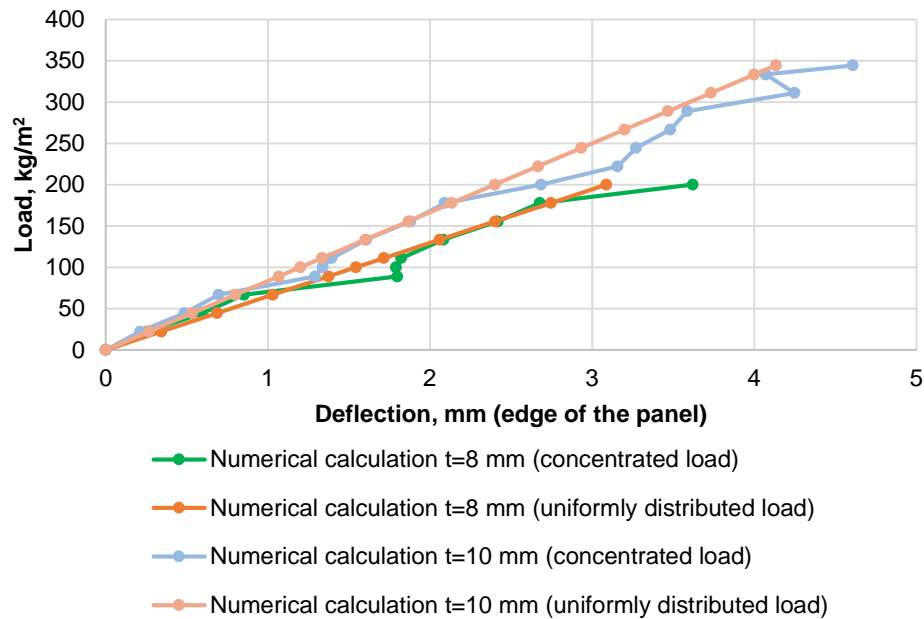Egorov, D., Galyamichev, A., Gerasimova, E., Serdjuks, D.

Figure 22. Deflection of the edge of the panel for the panels with the different thicknesses.

3.3. Verification of the cladding in terms of ULS

Major stresses arising in the plate under the action of a uniformly distributed load were calculated for evaluating the panel stress-strain state in accordance with ULS. The character of the stress distribution on the upper surface of the panel is shown in Fig. 23.
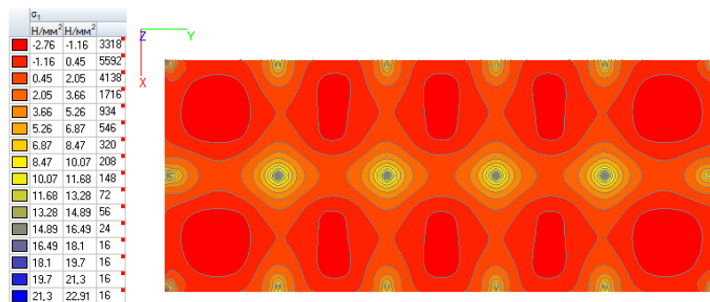

**Figure 23. Distribution character of major stresses σ_1
in the panel under uniformly distributed load, MPa.**

The ULS criteria for FCB is bending strength manufacturer's guideline:

$$R = 26.1\,MPa$$

Ultimate load acting on the panel and corresponding to the reaching of ULS (Table 1) was calculated according to Fig. 24, by linear interpolation of load and displacement values.
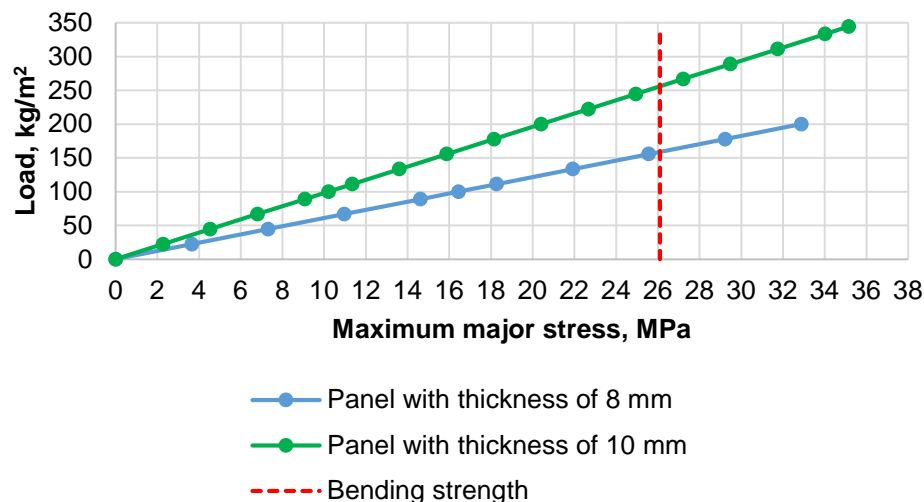

Figure 24. Maximum major stresses in the panel.

Table 1. Maximum allowable load in accordance with ULS requirements.

Panel thickness, mm	Load q_l, kg/m^2
8	158.8
10	255.9

3.4. Verification of the cladding in terms of SLS

The SLS criteria for FCB is its maximum allowable deflection determined in Russian Set of Rules 20.13330.2016 "Loads and actions" and equal to:

$$f_{SLS} = \frac{s}{150} \tag{3}$$

where s is minimum distance between fastening elements of the panel (rivets).

$$f_{SLS} = \frac{708}{150} = 4.72 \; mm$$

In the course of numerical modeling and experimental research, the displacements at characteristic points of the panel within the system were obtained. The final values consisted of joint deflections of the supporting frame and cladding.

For the correct stress-strain state assessment of FCB in accordance with SLS it is necessary to evaluate the deflections of cladding deforming independently. For this purpose, the numerical model of the FCB included cladding apart represented in the form of plate composed of shell finite elements and fixed by hinges at each position of fastening element (rivet) (Fig. 25). At the installation point, linear fixing was made to and from the plane of the facade panel.

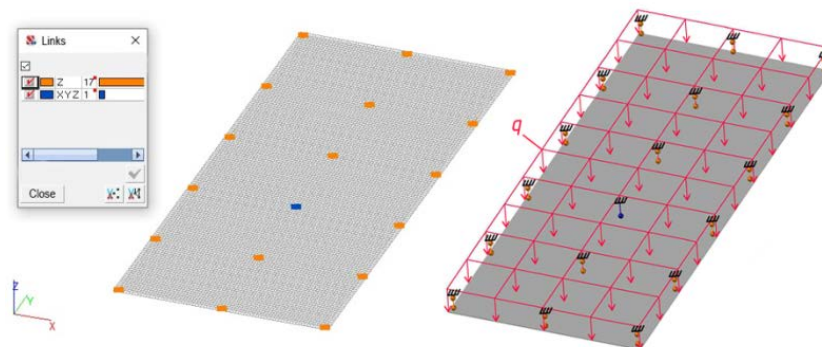Vertical movements of a panel under the action of uniformly distributed load are shown in Fig. 26.

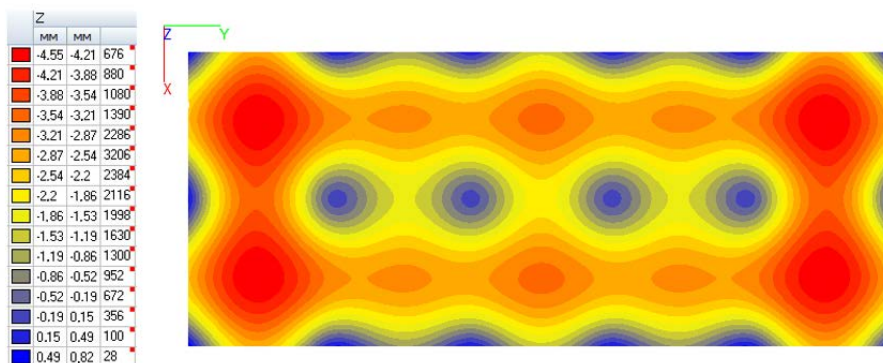**Figure 25. Structural scheme of the panel including fixing points and load application.**

**Figure 26. Displacement of the panel (t = 8 mm) in z-direction under the action
of uniformly distributed load of 88.89 kg/m^2.**

The maximum value of the load acting on the panel, which corresponded to the onset of SLS (Table 2), was calculated on the base of information provided in Fig. 27 by linear interpolation of the load and displacement values.
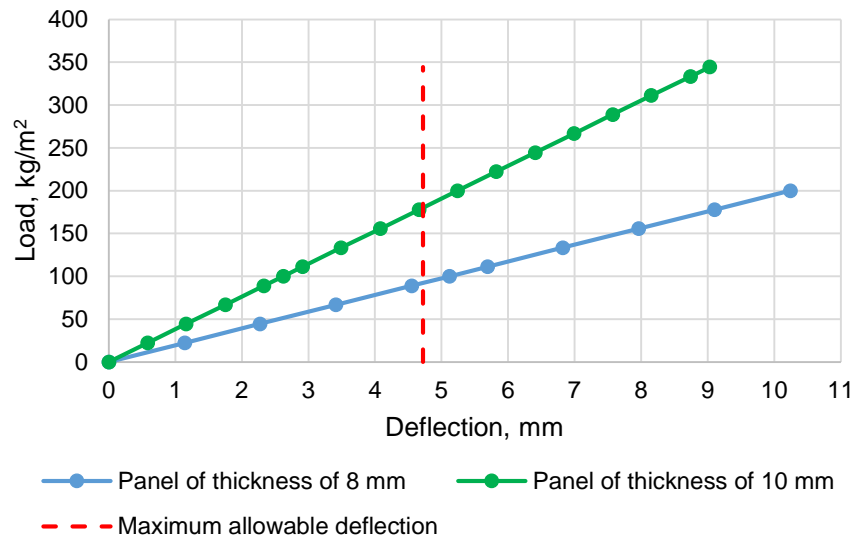
Figure 27. Deflections of the panel obtained through numerical modeling.

For the purpose of correct comparison of the maximum loads at the onset of the SLS and ULS and determination of defining state, a reduced (design) value is introduced for the case of SLS:

$$q_{SLS,SF} = q_{SLS} \cdot \gamma_f \tag{4}$$

where γ_f is safety factor, which is equal to 1.4 for the case of wind load.

Table 2. Maximum allowable load for SLS verification.

Panel thickness, mm	q_{SLS}, kg/m2	$q_{SLS,\ SF}$, kg/m2
8	92.2	129.1
10	181	253.4

3.5. Analysis and Discussion

Maximum vertical displacements of the center of the panel obtained during experimental study and numerical simulation are summarized in Fig. 28 and 29.
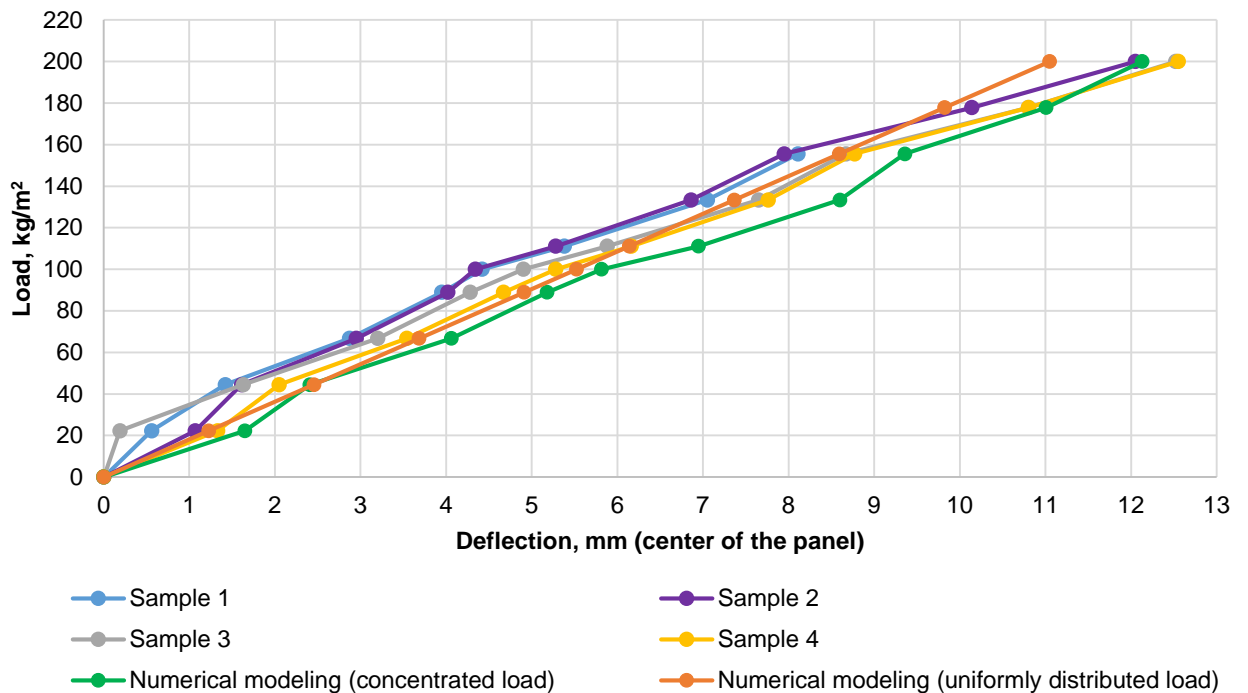

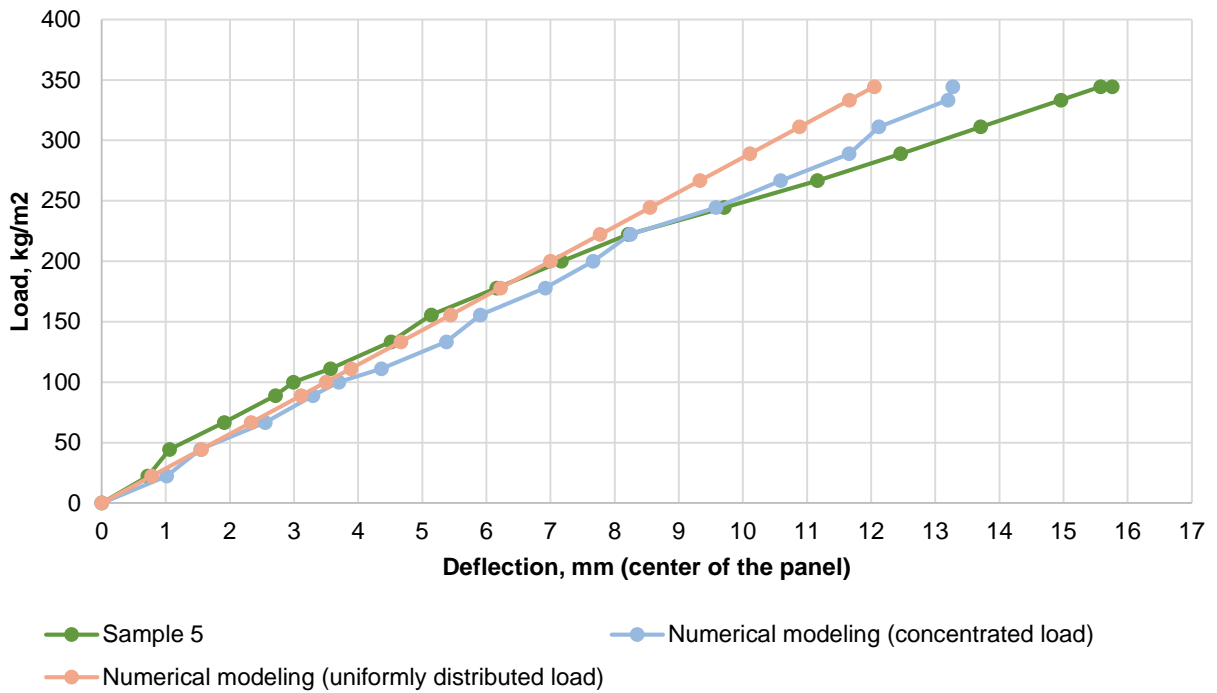**Figure 28. Deflection of the center of the panel (t = 8 mm).**

Figure 29. Deflection of the center of the panel (t = 10 mm).

Given that plastic deformations of subframe profile appear and increase near the area of its attachment to the supporting bracket, at certain load values displacements of the panel start to increase sharply (areas of convergence of numerical simulation and experimental research).

The dependence of the movements of the joint between central bracket and subframe profile on the acting load is shown in Fig. 30. When load increases the behavior of this connection changed from elastic to plastic as a result of local plastic deformations of the subframe profile, while in the numerical model it was realized through linear dependence of the displacements on the load by introducing elasto-plastic bonds.
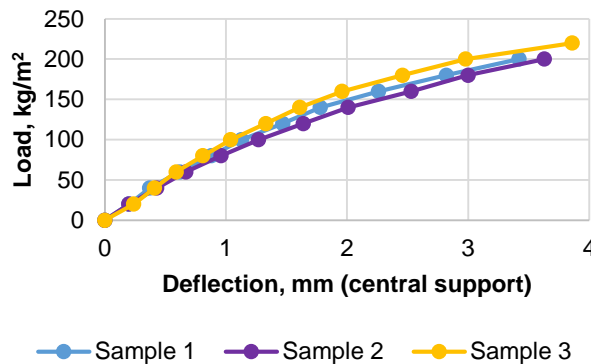

Figure 30. Dependence of the displacement of the joint between central bracket and subframe on the value of load acting on the panel.

According to the results of numerical modeling, loss of bearing capacity of the panel occurred due to the bending of the panel. Similarly, the loss of bearing capacity during the tests occurred due to formation of cracks in the area with the maximum value of bending stresses.

As the numerical modeling provides lower values of the system deflection in comparison with test results, it can be concluded that the design on the base of numerical simulation considered a margin of rigidity and verification of bearing capacity.

The maximum loads corresponding to the onset of ULS and SLS obtained during numerical simulation are shown in Table 3.

Table 3. Values of loads corresponding to the onset of ULS and SLS.

Panel thickness, mm	Maximum value q_{ULS}, kg/m²	Maximum value $q_{SLS, SF}$, kg/m²
8	158.8	129.1
10	255.9	253.4

Egorov, D., Galyamichev, A., Gerasimova, E., Serdjuks, D.

Existing researches, which were found and analyzed by authors within this study, did not have comprehensive information regarding stress-strain state of considered element under consimilar parameters and therefore final results could not be compared, however the design methods and main principles of calculation in accordance with Limit State design remain analogous.

4. Conclusions

FCBs fastened to the metal supporting frame of curtain wall system by exhaust rivets were analyzed within this study. The results obtained through experiments and numerical simulation allow to draw following conclusions:

1. Onset of Serviceability Limit State is critical verification for the design of the investigated type of FCBs.

2. A distance between fastening elements of FCBs equal to 750 mm and an edge distance of 30 mm are acceptable parameters in accordance with requirements arising from Ultimate Limit State design.

3. Onset of Ultimate Limit State is characterized by appearance of cracks due to the stresses in the panel exceeding the value of flexural strength in the area of fastening to curtain wall frame.

4. The profiles of the curtain wall system significantly affect performance of cladding panels and act as stiffening ribs of the FCB.

5. Linear formulation of Finite Element Method with careful consideration of boundary conditions can be used for determination of stress-strain state of FCBs.

6. The numerical calculation method provides a margin in verification of bearing capacity.

7. Accurate assessment of stress-strain state of both the cladding panel and the system as a whole requires calculation and accounting the stiffness of the joint between subframe and supporting bracket.

8. The stress-strain state of the cladding panel depends on the chosen frame of curtain wall system and its rigidity; therefore, cladding panels must be tested as a part of the system.

5. Acknowledgement

References

1. Mohr, B.J., El-Ashkar, N.H., Kurtis, K.E. Fiber-cement composites for housing construction: State-of-the-art review. Proceedings of the NSF Housing Research Agenda Workshop. Orlando, 2004. Pp. 112–128.

2. Mukhametrakhimov, R., Lukmanova, L. The Modified Fiber Cement Panels for Civil Construction. Advances in Intelligent Systems and Computing. 2018. No. 692. Pp. 852–858. DOI: 10.1007/978-3-319-70987-1_91

3. Lukmanova, L.V., Mukhametrakhimov, R.K., Gilmanshin, I.R. Investigation of mechanical properties of fiber-cement board reinforced with cellulosic fibers. IOP Conference Series: Materials Science and Engineering. 2019. 570 (1). DOI: 10.1088/1757-899X/570/1/012113

4. Mukhametrakhimov, R.Kh., Izotov, V.S. Povysheniye fiziko-mekhanicheskikh svoystv i dolgovechnosti fibrotsementnykh plit na osnove tsellyuloznykh volokon [Improvement of physico-mechanical properties and durability of fiber cement boards based on cellulose fibers]. Izvestiya vuzov. Stroitelstvo. 2012. No. 9. Pp. 101–107. (rus).

5. Sonphuak, W., Rojanarowan, N. Strength improvement of fibre cement product. International Journal of Industrial Engineering Computations. 2013. 4 (4). Pp. 505–516. DOI: 10.5267/j.ijiec.2013.06.004

6. ACI Committee 544. "State-of-the-Art Report on Fiber Reinforced Concrete". American Concrete Institute. 1973. 70 (11). Pp. 729-744.

7. Melcher, J., Karmazínová, M., Pilgr, M. Evaluation of strength characteristics of fibre-cement slab material. Advanced Materials Research. 2013. No. 650. Pp. 320–325. DOI: 10.4028/www.scientific.net/AMR.650.320

8. Gorzelańczyk, T., Schabowicz, K. Effect of freeze-thaw cycling on the failure of fibre-cement boards, assessed using acoustic emission method and artificial neural network. Materials. 2019. 12 (13). DOI: 10.3390/ma12132181

9. Ranachowski, Z., Ranachowski, P., Debowski, T., Gorzelańczyk, T., Schabowicz, K. Investigation of structural degradation of fiber cement boards due to thermal impact. Materials. 2019. 16 (6). DOI: 10.3390/ma12060944

10. Jamshidi, M., Pakravan, H.R., Pacheco-Torgal, F. Assessment of the Durability Performance of Fiber-Cement Sheets. Journal of Materials in Civil Engineering. 2013. 25 (6). Pp. 819–823. DOI: 10.1061/(ASCE)MT.1943-5533.0000637

11. Adamczak-Bugno, A., Swit, G., Krampikowska, A. Assessment of Destruction Processes in Fibre-Cement Composites Using the Acoustic Emission Method and Wavelet Analysis. IOP Conference Series: Materials Science and Engineering. 2019. 471 (3). DOI: 10.1088/1757-899X/471/3/032042

12. Kondratyeva, N.V. Prochnost i deformativnost konstruktsiy iz listovogo stekla pri poperechnom izgibe ravnomerno raspredelennoy nagruzkoy [Strength and deformability of sheet glass structures under transverse bending by uniformly distributed load]. PhD Thesis. Samara State University of Architecture, Building and Civil Engineering. 2010. 176 p. (rus)

13. Galyamichev, A.V., Alkhimenko, A.I. Design features of facade cassettes from thin ceramics. Magazine of Civil Engineering. 2017. 69 (1). Pp. 64–76. DOI: 10.18720/MCE.69.6

14. Schmid, P., Daněk, P., Rozsypalová, I., Holomek, P., Juránek, P. Assessment of the resistance of ventilated facade system by vacuum testing. IOP Conference Series: Materials Science and Engineering. 2019. 549 (1). DOI: 10.1088/1757-899X/549/1/012034

15. Antonov, A.S., Shmelev, G.N., Sabitov, L.S., Kashapov, N.F., Galimullin, I.A. Study of the real work of constructions of translucent facade systems. IOP Conference Series: Materials Science and Engineering. 2019. 570 (1). DOI: 10.1088/1757-899X/570/1/012006

16. Galyamichev, A.V. Spetsifika opredeleniya nagruzok na ograzhdayushchiye konstruktsii i yeye vliyaniye na rezultaty ikh staticheskogo rascheta [Specifics of determining loads on building envelopes and its effect on the results of static calculation]. Internet-zhurnal «NAUKOVEDENIE». 2015. 2 (27). (rus). DOI: 10.15862/54TVN215

17. Galyamichev, A.V. Vetrovaya nagruzka i yeye deystviye na fasadnyye konstruktsii. Stroitelstvo unikalnykh zdaniy i sooruzheniy [Wind load and its effect on facade structures]. 2017. 9 (60). Pp. 44–57. (rus). DOI: 10.18720/CUBS.60.4

18. Lalin, V.V., Rybakov, V.A. The finite elements for design of building walling made of thin-walled beams. Magazine of Civil Engineering. 2011. 26 (8). Pp. 69−80. (rus). DOI: 10.5862/MCE.26.11

19. Rybakov, V.A., Kozinetc, K.G., Vatin, N.I., Velichkin, V.Z., Korsun, V.I. Lightweight steel concrete structures technology with foam fiber-cement sheets. Magazine of Civil Engineering. 2018. 82 (6). Pp. 103–111. DOI: 10.18720/MCE.82.10

20. Ivanova, E., Strakhov, D., Sinyakov, L., Zimin, S. Joint work of steel floor beams and vaults. Construction of Unique Buildings and Structures. 2018. 10 (73). Pp. 7−15. DOI: 10.18720/CUBS.73.1

Contacts:

Denis Egorov, egorov.dv@edu.spbstu.ru

Alexander Galyamichev, gav@spbstu.ru

Ekaterina Gerasimova, katyageras17@gmail.com

Dmitrijs Serdjuks, Dmitrijs.Serdjuks@rtu.lv